

# **An Inductive Technique for Electrical Conductivity Measurements on Molten Metals<sup>1</sup>**

**S. G. Teodorescu,<sup>2</sup> R. A. Overfelt,<sup>2</sup> and S. I. Bakhtiyarov<sup>2, 3</sup>**

---

A computer-controlled rotational technique to measure the electrical resistivity of solid and molten metals was developed. The electrical resistivities of pure metals (aluminum, indium, lead, and tin) and the low-melting point alloy LMA-158 in the solid and liquid states were measured. The results also show that there is a linear relationship between electrical resistivity and temperature in both the solid and the liquid states of the test materials. Good agreement was found between the experimental data and predictions from the literature. The data were used to estimate the temperature coefficients of electrical resistivity of test specimens over a wide range of temperatures including the melting point of the metals. Good agreement between experimental data and predictions made by previous researchers for the temperature coefficients was achieved.

---

**KEY WORDS:** aluminum; electrical conductivity; inductive method; lead; molten metal; tin.

## **1. INTRODUCTION**

The optimization and control of metallurgical processes require the knowledge of many physical properties (e.g., viscosity, electrical conductivity, density, surface tension) of metals in the liquid state. Electrical conductivity is a basic physical parameter in the evaluation and design of new alloys and provides valuable information on the structure of molten metals in many metallurgical processes such as electroslug remelting and electromagnetic stirring in continuous and centrifugal castings.

---

<sup>1</sup> Paper presented at the Fourteenth Symposium on Thermophysical Properties, June 25–30, 2000, Boulder, Colorado, U.S.A.

<sup>2</sup> Department of Mechanical Engineering, 201 Ross Hall, Auburn University, Auburn, Alabama 36849-5341, U.S.A.

<sup>3</sup> To whom correspondence should be addressed. E-mail: sayavurb@eng.auburn.edu

By virtue of a disordered arrangement of ions, metals in a liquid state have a higher (by a factor of 1.5 to 2.3) electrical resistivity than solid metals with a regular arrangement of ions. The decrease in electrical conductivity is caused by the shortening of the electron mean free path when they are moving through the disordered liquid state [1]. The vibrating atoms model [2], the free-electron model [3, 4], and the fluctuation scattering theory [5, 6] are three main theories which allow predictions of the electrical conductivity of molten metals. The electrical conductivity predicted by these theories is in good agreement with experimental data obtained by different researchers.

Braunbeck [7] proposed the following relationship between the electric conductivity ( $\sigma_e$ ) of the specimen and the mechanical moment caused by mutual interaction between the external magnetic field and an additional magnetic field induced by the eddy current:

$$M = \frac{\pi}{4} \sigma_e \omega L R^4 B^2 - \frac{\pi}{192\eta} \sigma_e^2 \omega L R^6 B^4 \quad (1)$$

where  $M$  is the mechanical moment caused by mutual interaction between the external magnetic field and an additional magnetic field induced by the eddy current;  $L$  and  $R$  are the length and radius of the specimen, respectively;  $\omega$  is the angular velocity of the rotating magnetic field;  $B$  is the magnetic induction; and  $\eta$  is the viscosity of the liquid specimen.

According to Ref. 8, the magnetic induction and the dimensions of the specimen can be selected so that the second term in Eq. (1) may become negligibly small compared with the first term in the case of metals of unknown viscosity.

The methods of electrical conductivity measurements can be categorized into two groups:

- direct resistance measurements and
- contactless inductive measurements.

In direct resistance measurement techniques, high-melting noble metals (platinum, molybdenum, etc.) are used as electrodes. In aggressive metal melts they are subject to solution attack. Therefore, these methods are applicable for poor conductors and for calibration of the contactless inductive technique.

As a direct technique, the four-probe potentiometric method has been developed to measure the electrical conductivity of molten metals [9, 10]. In this method, at a constant current density the potential drop across the molten sample in a capillary tube of a known cross section and length is

measured. The probe cell has to be calibrated using a liquid metal (usually mercury) of known electrical conductivity. Selection of the proper material for the capillary cell and the electrodes is a major problem in this method. Dissolution of electrodes and chemical reaction between them may occur. Hence, an improved four-probe method has since been developed [11]. This method uses solid electrodes made of identical material to the molten sample.

The contactless inductive measurement technique excludes the dissolution, chemical reaction, and contact resistance phenomena. The method is based on the phenomenon that when a metal sample moves in a magnetic field (or a magnetic field rotates around the sample), circulating eddy currents are induced in the sample. These currents generate a damping torque proportional to the electrical conductivity of the sample. In liquid metals and alloys the applied magnetic field causes liquid circulation in the crucible. Consequently, it results in a decrease in the velocity of induced eddy currents. The rotating magnetic field method to measure the electrical conductivity of molten metals and alloys was used in Refs. 12–14. The advantage of the method is the possibility of measuring at the same time the viscosity of the molten sample by the damping of the torsional oscillation of the cell [15].

The capillary technique was been used in Refs. 16 and 17 to measure the electric conductivity of the lead–tin binary system. The rotational technique was used in Refs. 18–20. There is good agreement between the data obtained by rotational techniques. However, the data obtained by the capillary techniques disagreed among themselves and with data obtained by rotational methods. Ozelton and Wilson [20] assume that the capillary method is affected by the separation of the constituents (liquid and solid) of the alloy by the direct electric current passage.

The objective of this work is to design a contactless inductive technique (with a metal sample moving in a magnetic field) for measuring the electrical resistivity of solid and liquid metals. This paper presents some preliminary results for pure metals and a low melting point alloy over a wide range of temperatures.

## **2. TEST MATERIALS, EXPERIMENTAL APPARATUS, AND PROCEDURE**

Schematics of the experimental setups to measure the electrical conductivity of metals and alloys at high temperatures are illustrated in Figs. 1 and 2. A computer-controlled Brookfield rheometer (Model DV-III) was used to provide a constant rotational speed to the metal sample and to measure the torque precisely. This rheometer allows torque measurements

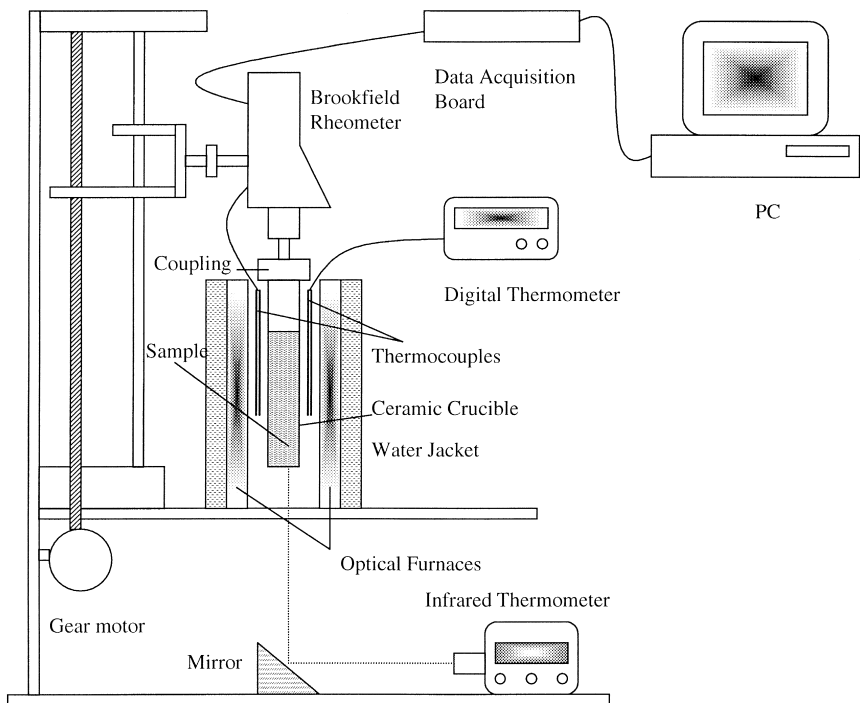


**Fig. 1.** The experimental apparatus used for electrical conductivity measurements of solid and molten metals.

(0 to  $6.7 \times 10^{-7}$  N·m) at constant speeds from 0 to 250 rpm in 0.1-rpm increments.

The temperature of the sample has been measured simultaneously with three thermocouples. The temperature probe DVP-28Y was connected to the computer, and data obtained were synchronized with data for measured torque and angular velocity of crucible. The outputs of two other thermocouples were coupled to a Digital Temperature Indicator. The thermocouples were calibrated against the melting points of pure lead and tin. In addition, a Micron infrared thermometer was used to measure the temperature at the crucible surface.

The metal sample was placed inside the flat-bottomed cylindrical, extruded, high-purity alumina crucible attached to the spindle of the rheometer through a specially designed coupling system to provide a concentricity to the rotating crucible with the sample. Alumina crucibles (9.525-mm diameter and 152.4-mm length) with samples of the same diameter and 38.1-mm length were exposed to the magnetic field and heating. During

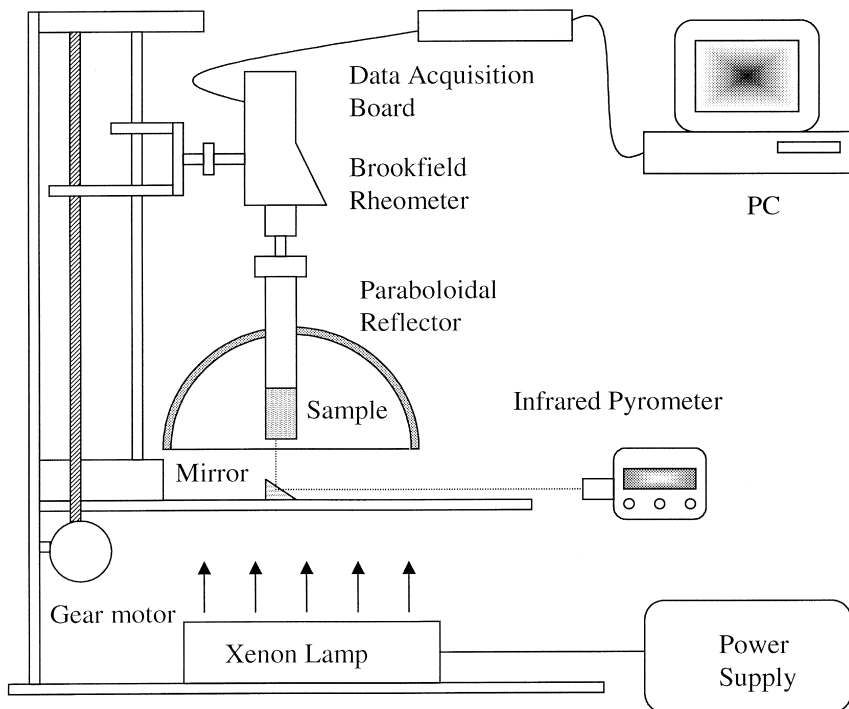


**Fig. 2.** The experimental apparatus with the paraboloidal reflector furnace used for electrical conductivity measurements of solid and molten metals.

each set of tests it was essential to maintain the sample length constant. For each metal sample the mass was determined according to the required size of the sample and density.

The motor driven 3D positioning system was designed and fabricated to provide high accuracy positioning to the crucible with the sample, heating elements, magnets, and infrared thermometer. The gear motor, with a maximum speed of 500 rpm, was used in the positioning system to provide low-speed variations (0.1%).

Quartz infrared line heating elements housed in elliptical cast aluminum frames were used as a furnace in the experimental apparatus shown in Fig. 1. The heated length of the chamber is 167 mm. The elliptical reflectors provide concentrated infrared energy to the test specimen. High-density infrared energy is produced by tubular, high temperature quartz lamps (Q2000T4/CL) with tungsten-wire filament emitters. The lamps supply energy (2 kW each) in the infrared region above the visible range in the electromagnetic spectrum and are housed in an array of elliptical

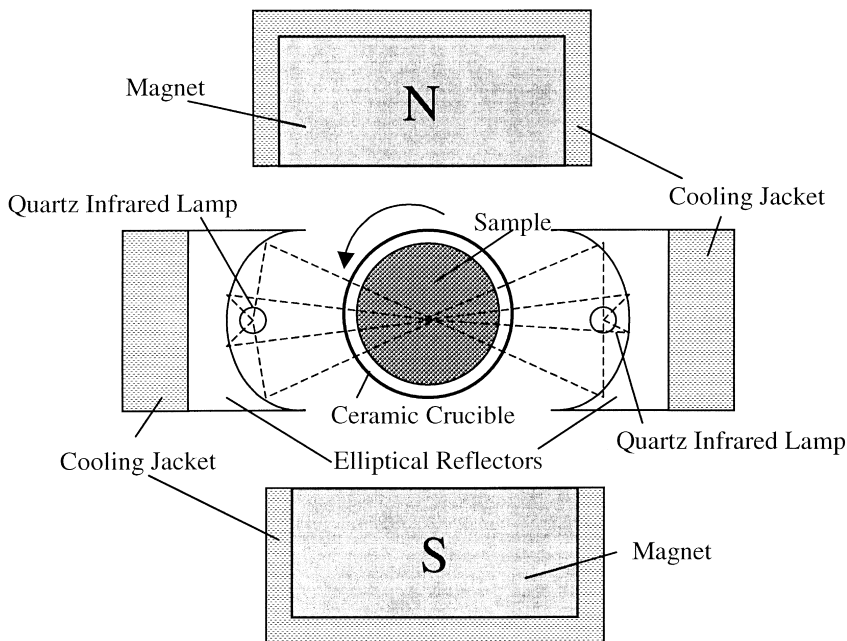


**Fig. 3.** Diagram of the sample-magnetic field-optical furnace arrangement and heating energy focus action.

reflectors. The reflectors focus infrared energy from the lamps on the specimen (Fig. 3). The full voltage temperature output is 2980°C. Copper tube connections are provided for inlet and outlet flow of coolant (water) to cool the lamp reflector bodies. Tap water at 15°C and 600 kPa was supplied to cool the unit.

In the experimental technique presented in Fig. 2, a paraboloidal reflector was used to capture the light sent by the 5-kW xenon lamp coated with bright rhodium. The light was focused on the point located 60 mm below the top. The auto-shutoff relay was incorporated inside the power supply and allowed heating of the sample for ~10 min. The internal blower cooled the lamp.

The magnetic field was generated by two neodymium permanent magnets. An MG-4D gaussmeter (Walker Scientific Inc.) operating on the Hall-effect principle was used to measure the magnetic field strength. It provides dc and ac field readings from  $\pm 10^{-5}$  to  $\pm 2$  T with 0.1% resolution. By changing the distance between the magnets, we could obtain a magnetic field of desirable strength. It was important to obtain a magnetic field with uniformly distributed induction. Mapping performed by the

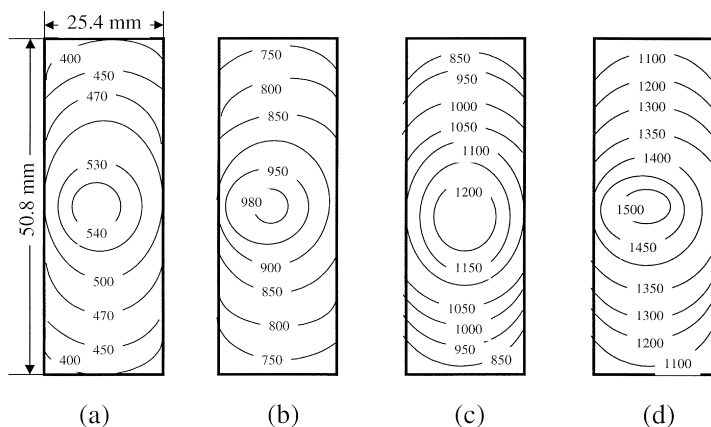


Fig. 4. Contour lines for magnetic induction (in  $10^4$  T) at different distances between magnets: (a) 12 cm; (b) 9 cm; (c) 8 cm; (d) 7 cm.

MG-4D gaussmeter revealed that the magnetic induction varies in both the vertical and the horizontal directions. Contour lines for the magnetic induction at different distances between the magnets are shown in Fig. 4. Estimations indicate that the magnetic induction over the test sample varies  $\pm 10\%$  in the vertical direction and  $\pm 7\%$  in the horizontal direction compared to its average value. Figure 5 shows the variation of the magnetic induction with the distance between the magnets. Neither the coupling system nor the alumina crucible had perceptible disturbing effects on the applied magnetic field.

As a test sample we used aluminum of 99.999% purity, indium (99.99%), lead (99.9999%), tin (99.999%) and a low-melting alloy LMA-158. The composition of this alloy and some thermophysical properties of the components in the liquid state are listed in Table I. The electrical resistance of the solid samples was also measured using a 4300B digital microohmmeter (Valhalla Scientific, Inc.). The Kelvin four-terminal configuration of this ohmmeter eliminates errors caused by the test lead and contact resistance which, in many applications, can exceed the value of the load by several orders of magnitude.

### 3. RESULTS AND DISCUSSION

The effect of the induced magnetic field is characterized by the magnetic Reynolds number, defined as

$$\text{Re}_m = \omega \sigma_c \mu_0 R^2 \quad (2)$$

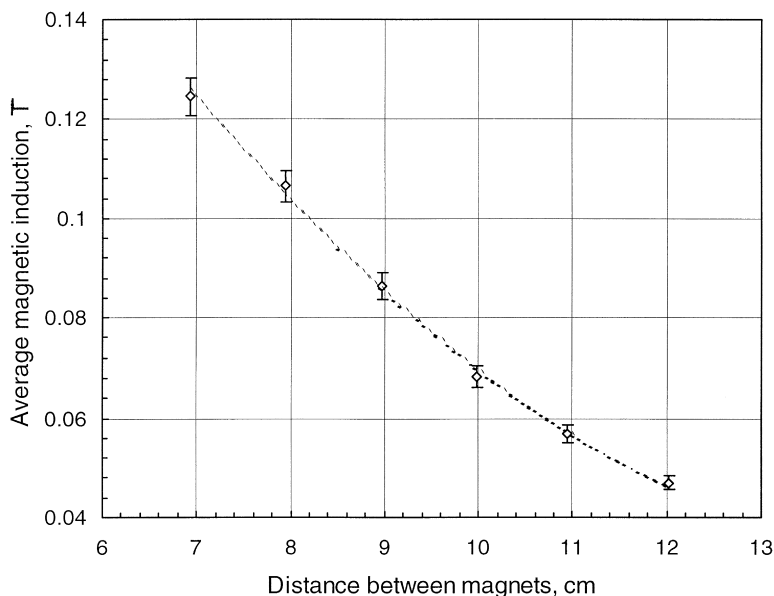


Fig. 5. Variation of the averaged magnetic induction with the distance between magnets.

where  $\mu_0$  is the magnetic permeability. Simulations show that in our experiments  $Re_m \ll 1$ , which means that the magnetic field distribution is not affected by the fluid motion and may be evaluated as though the conducting liquid were a solid. Also, the induction of an electric field by fluctuations of the magnetic field can be disregarded in comparison with the electromagnetic force.

Table I. LMA-158 Components and Their Thermophysical Properties in the Liquid State [1]

LMA-158 component	Weight (%)	Melting Point (K)	Density ( $\text{g} \cdot \text{cm}^{-3}$ )	Electrical resistivity ( $\mu\Omega \cdot \text{cm}$ )	Viscosity ( $\text{mPa} \cdot \text{s}$ )
Bismuth	50.0	544.1	10.05	130.2	1.63
Lead	26.7	600.55	10.67	95	2.61
Tin	13.3	504.99	6.98	48	1.81
Cadmium	10.0	594.05	8.01	33.7	2.60



The flow regime of the melt flow in the rotating cylindrical container is determined by the hydraulic Reynolds number, which represents the ratio of inertia forces to viscous forces, and is defined by the formula

$$\text{Re} = \frac{\omega R^2 \rho}{\mu} \quad (3)$$

where  $\mu$  and  $\rho$  are the shear viscosity and density of the liquid metal, respectively, and  $\omega$  is the angular velocity of fluid rotation. The calculations of the Reynolds numbers for lead, tin, and aluminum under test conditions show that the flow regime in the container for all samples is laminar.

First, the damping torque was calibrated against the electrical resistivity of pure lead and tin. The damping torque, and hence the electrical resistivity, increases with increases in the sample length. Thus, one would assume a significant contribution of end effects on the measured values of the damping torque. The effects can be eliminated from the results of two experiments accomplished with different heights (24.5 and 36.75 mm) of the test sample in the crucible but at the same angular speed ( $\omega = 35$  rpm) and

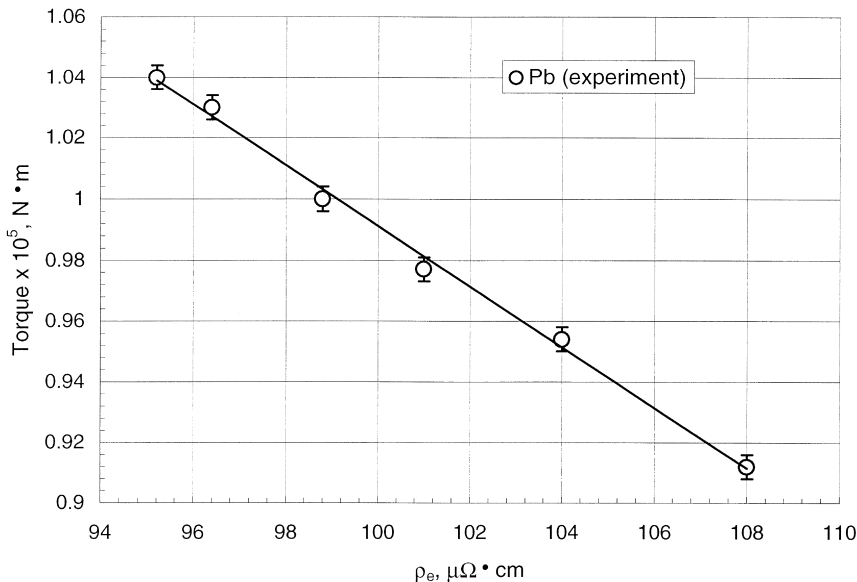


**Fig. 6.** Calibration of damping torque for liquid lead at  $\omega = 35$  rpm and  $B = 0.1$  T. Solid lines correspond to simulations by Eq. (1).

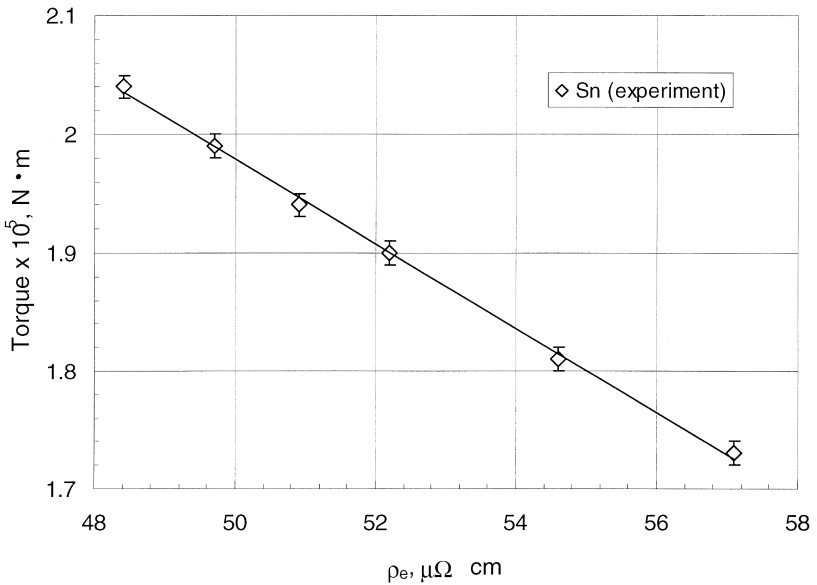


Fig. 7. Calibration of damping torque for liquid tin at  $\omega = 35$  rpm and  $B = 0.1$  T. Solid lines correspond to simulations by Eq. (1).

diameter (19.2 mm). Calibration results with elimination of the end effects are shown in Figs. 6 and 7 along with simulation results by Eq. (1) for lead and tin, respectively. There is good agreement between calibration data and predictions.

The variation of the damping torque, caused by the induced circular eddy currents, for aluminum, indium, lead and tin samples, with the angular velocity at different temperatures is shown in Fig. 8. The damping torque decreases with temperature at a fixed angular speed ( $\omega = 35$  rpm) and magnetic induction ( $B = 0.1$  T). As shown in Fig. 8, at the melting points of the test samples, the torque decreases dramatically as a result of weak eddy currents for samples in the liquid phase.

Figure 9 represents a variation of the electrical resistivity of the test samples in both the solid and the liquid states versus temperature. The data are in good agreement with results from the literature.

The electrical resistivity of LMA-158 alloy as a function of temperature is represented in Fig. 10. At the melting point ( $T = 70^\circ\text{C}$ ) of the alloy the electrical resistivity increases by almost a factor of two. The results also show that there is a linear relationship between electrical resistivity and temperature for both the solid and the liquid states of the alloy.

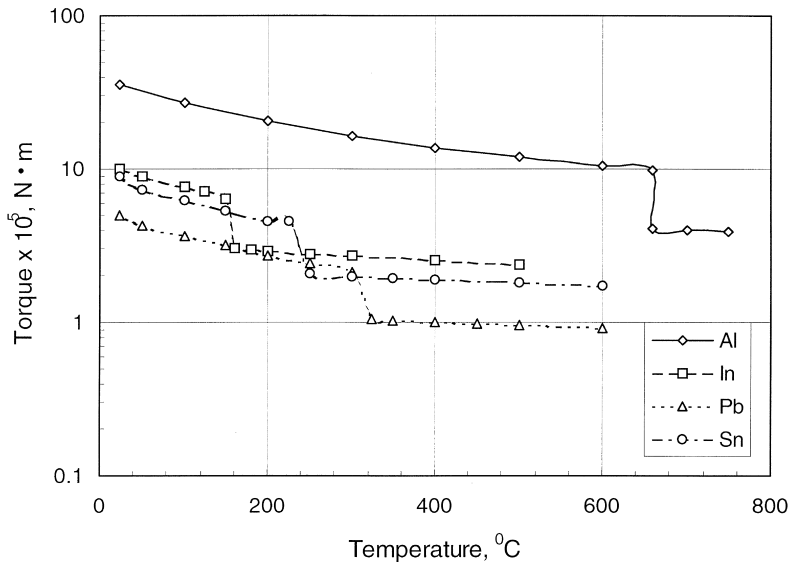


Fig. 8. Variation of damping torque with temperature for aluminum, indium, lead, and tin in the solid and liquid states ( $\omega = 35 \text{ rpm}$  and  $B = 0.1 \text{ T}$ ).

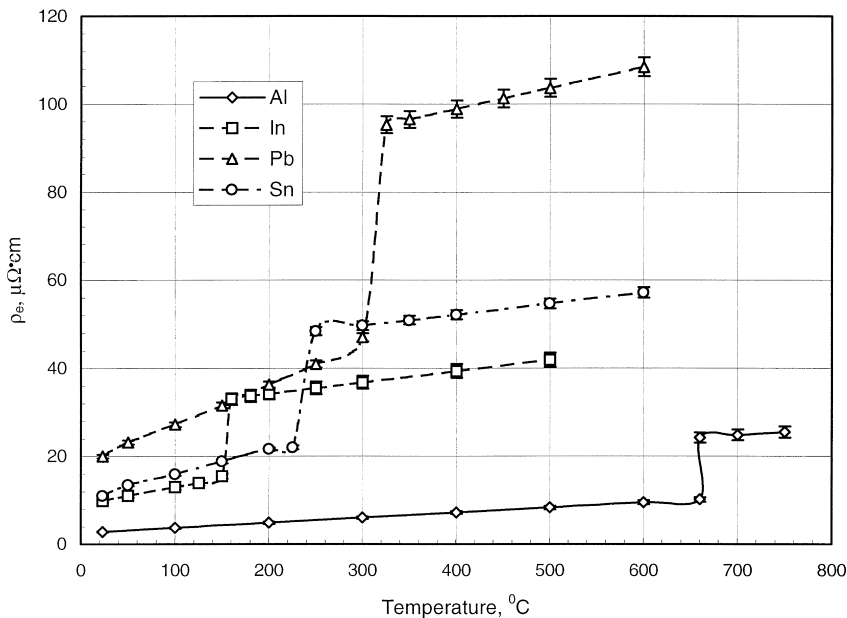
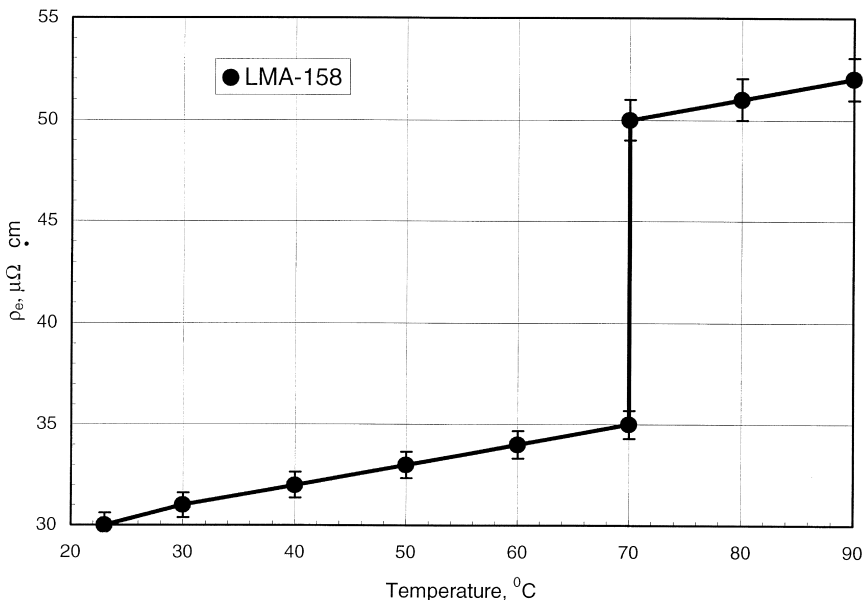


Fig. 9. Variation of electrical resistivity with temperature for aluminum, indium, lead, and tin in the solid and liquid states ( $\omega = 35 \text{ rpm}$  and  $B = 0.1 \text{ T}$ ).



**Fig. 10.** Variation of electrical resistivity of LMA-158 alloy with temperature at  $\omega = 35$  rpm and  $B = 0.1$  T.

It is well known that the change in the electrical resistance of conductor materials in both the solid and the liquid phases is proportional to the change in temperature. The electrical resistivity of liquid metals increases linearly with increasing temperature (except for Cd and Zn) [1]. This relationship can be expressed as

$$\rho_e = \alpha T + \beta \quad (4)$$

where  $\alpha$  and  $\beta$  are temperature coefficients of the electrical resistivity for liquid metals.

The measured values of the temperature coefficients ( $\alpha$  and  $\beta$ ) of resistivity for molten aluminum, indium, lead, tin, and LMA-158 alloy samples at different temperatures are presented in Figs. 11 and 12. The lines denote the values of these coefficients proposed in Ref. 21. As is apparent, there is adequate agreement between the measured and the proposed values of both temperature coefficients (with a deviation of  $\pm 5\%$ ).

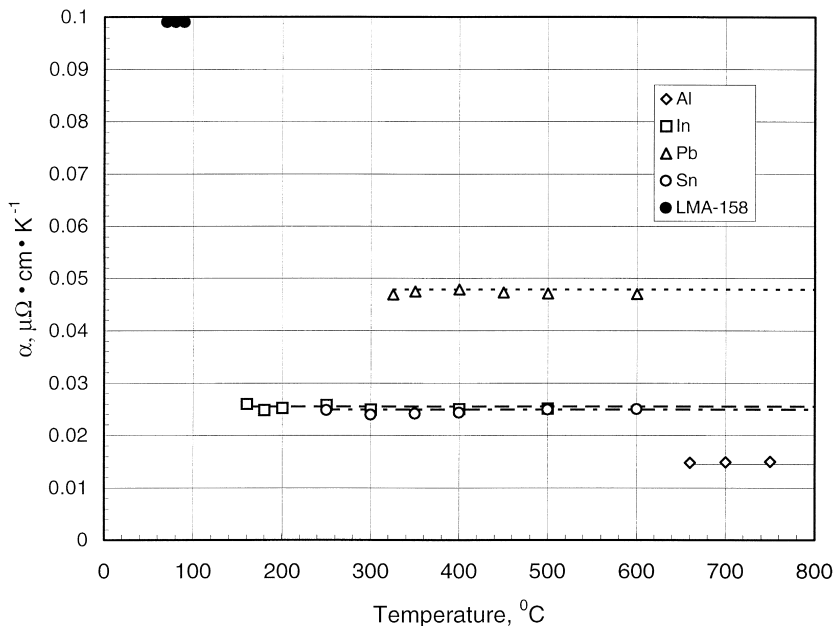
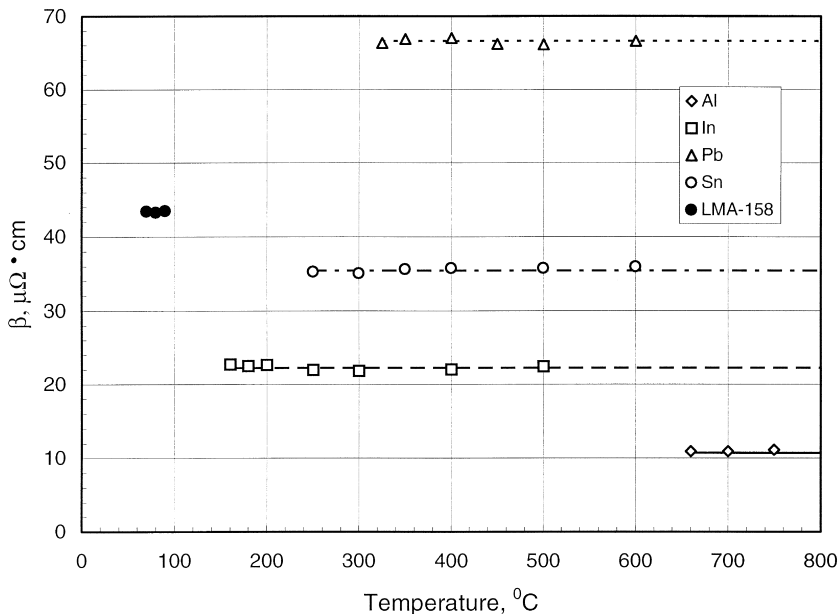


Fig. 11. Variation of the temperature coefficient  $\alpha$  with temperature for liquid aluminum, indium, lead, tin, and LMA-158 alloy ( $\omega = 35$  rpm and  $B = 0.1$  T). Lines denote predictions of Ref. 21.

#### 4. CONCLUSIONS

A contactless inductive rotational technique to measure the electrical resistivity of solid and molten metals was developed. Furnaces with the elliptical and paraboloidal reflectors were used to melt the metal samples. The damping torque was calibrated against the electrical resistivity of pure lead and tin. The end effects were eliminated from the results of two experiments by using different lengths of the test sample in the crucible but the same angular speed and sample diameter. The electrical resistivities of the pure metals (aluminum, indium, lead, and tin) and the low-melting point alloy LMA-158 for the solid and liquid states were measured. The results show that there is a linear relationship between electrical resistivity and temperature for both the solid and the liquid states of the test materials. Good agreement was found between our experimental data and the predictions of Braunbeck [7].

The data were used to estimate the temperature coefficients of electrical resistivity of test specimens over a wide range of temperature including



**Fig. 12.** Variation of the temperature coefficient  $\beta$  with temperature for liquid aluminum, indium, lead, tin, and LMA-158 alloy ( $\omega = 35$  rpm and  $B = 0.1$  T). Lines denote predictions of Ref. 21.

the melting points of the metals. Good agreement between experimental data and predictions by previous researchers was achieved.

## ACKNOWLEDGMENT

The authors gratefully acknowledge the financial support received from NASA's Office of Life and Microgravity Sciences and Applications under Cooperative Agreement No. NCC8-128.

## REFERENCES

1. T. Iida and R. I. L. Guthrie, *The Physical Properties of Liquid Metals* (Clarendon Press, Oxford, 1988).
2. N. F. Mott, *Proc. Roy. Soc.* **A146**:465 (1934).
3. J. M. Ziman, *Phil. Mag.* **6**:1013 (1961).
4. R. Evans, D. A. Greenwood, and P. Lloyd, *Phys. Lett.* **35A**:57 (1971).
5. S. Takeuchi and H. Endo, *J. Japan Inst. Metals* **26**:498 (1962).
6. J. L. Tomlinson and B. D. Lichter, *Trans. Met. Soc. AIME* **245**:2261 (1969).
7. W. Braunbeck, *Z. Phys.* **3**:312 (1932).

8. S. Takeuchi and H. Endo, *Trans. Japan Inst. Metals* **3**:30 (1962).
9. P. D. Adams and J. S. Leach, *Phys. Rev.* **156**:178 (1967).
10. Y. Mera, Y. Kita, and A. Adachi, *Tech. Rep. Osaka Univ.* **22**:445 (1972).
11. G. S. Ershov, A. A. Kasatkin, and I. V. Gavrilin, *Izv. Akad. Nauk SSSR Metall* **2**:98 (1976).
12. A. M. Samarin, *J. Iron Steel Inst.* **200**:95 (1962).
13. Y. Ono and T. Yagi, *Trans. ISIJ* **12**:314 (1972).
14. S. I. Bakhtiyarov and R. A. Overfelt, *J. Mater. Sci.* **34**:945 (1999).
15. S. I. Bakhtiyarov and R. A. Overfelt, *Acta Mater.* **47**:4311 (1999).
16. T. C. Toye and E. E. Jones, *Proc. Phys. Soc.* **71**:88 (1958).
17. A. M. Korolkov and D. P. Shashkov, *Izv. Akad. Nauk. SSSR Met. Topl.* **1**:84 (1962).
18. A. Roll and G. Fees, *Z. Metall.* **51**:540 (1960).
19. S. Takeuchi and H. Endo, *Trans. Japan Inst. Metals* **3**:35 (1962).
20. M. W. Ozelton and J. R. Wilson, *J. Sci. Instrum.* **43**:359 (1966).
21. N. Cusack and J. E. Enderby, *Proc. Phys. Soc.* **75**:395 (1960).